Reported Anatomical Variability Naturally Leads to Multimodal Distributions of Denavit-Hartenberg Parameters for the Human Thumb

Veronica J. Santos, *Member, IEEE* and Francisco J. Valero-Cuevas*, *Member, IEEE*

Abstract—A realistic biomechanical thumb model would elucidate the functional consequences of orthopedic and neurological diseases and their treatments. We investigated whether a single parametric kinematic model can represent all thumbs, or whether different kinematic model structures are needed to represent different thumbs. We used Monte Carlo simulations to convert the anatomical variability in the kinematic model parameters into distributions of Denavit–Hartenberg parameters amenable for robotics-based models. Upon convergence (3550 simulations, where mean and coefficient of variance changed $< 1\%$ for the last $20 + \%$ simulations) the distributions of Denavit-Hartenberg parameters appeared multimodal, in contrast to the reported unimodal distributions of the anatomy-based parameters. Cluster analysis and one-way analysis of variance confirmed four types of kinematic models ($p < 0.0001$) differentiated primarily by the biomechanically relevant order of MCP joint axes (in 65.2% of models, the flexion-extension axis was distal to the adduction-abduction axis); and secondarily by a detail specifying the direction of a common normal between successive axes of rotation. Importantly, this stochastic analysis of anatomical variability redefines the debate on whether a single generic biomechanical model can represent the entire population, or if subject-specific models are necessary. We suggest a practical third alternative: that anatomical and functional variability can be captured by a finite set of model-types.

Index Terms—Biomechanical model, biorobotics, hand, kinematics, stochastic simulation, thumb.

I. INTRODUCTION

FROM the most precise pinch to the most powerful grasp, the functional versatility of the human thumb is evident whenever we use our hands to interact with objects. This versatility is all the more impressive when we consider that hand anatomy varies across individuals, leading to questions about how different hands will respond to the same clinical treatment, or how the nervous system adapts to control different hands. To

date, little attention has been paid to the functional and clinical consequences of anatomical variability in general, and thumb variability in particular.

Realistic biomechanical models are a means to study the functional consequences of anatomical variability. In a prior Monte Carlo study, we found that approximating the kinematic structure of the thumb with hinged linkages with universal joints (i.e., orthogonal and intersecting axes of rotation) at the carpometacarpal (CMC) and metacarpophalangeal (MCP) articulations cannot realistically predict three-dimensional (3-D) static thumbtip forces—likely because they do not realistically transform net joint torques into thumbtip forces and torques [1]. This finding motivates us to explore the more complex alternative of approximating thumb kinematic structure with generic hinged linkages with nonintersecting, nonorthogonal axes of rotation [2], [3]. This "virtual five-link" description, inferred from studies performed on seven cadaveric thumbs, represents the thumb kinematic structure as a serial chain of five hinges in which the two axes of rotation [flexion-extension (FE) and adduction-abduction (AA) rotational degrees of freedom (DOF)] at the CMC and MCP joints are not mutually orthogonal or intersecting [4]. As in our previous work, the interphalangeal (IP) joint has one axis of rotation for FE, and a single hinge connects successive virtual links to one another. The links of this model are called "virtual" because they correspond to the distance between consecutive effective hinges, and not simply the lengths of the thumb bones, as in simpler models. Importantly, however, the reported parameters of this anatomy-based description have large inter-subject variability and, in their current form, are not amenable for use in robotics-based biomechanical models.

As part of our efforts to create a realistic model of the thumb, we investigated whether a single parametric kinematic model can represent all thumbs, or whether different kinematic model structures are needed to represent different thumbs. We did so by converting the only available anatomy-based description of the kinematic structure of the thumb [4] into a standard robotics notation [Denavit-Hartenberg (D-H)] for use in robotics-based musculoskeletal models. To incorporate the effects of reported anatomical variability on kinematic structure of the thumb, we used Monte Carlo simulations because they explicitly incorporate the reported anatomical variability and measurement uncertainty in kinematic model parameters into the conversion to D-H notation. In addition, the Monte Carlo approach yields statistical distributions for the D-H parameters that emerge naturally from statistical distributions of the anatomical data.

II. METHODOLOGY

Our conversion of the anatomy-based kinematic model of the thumb into statistical distributions of D-H parameters consisted of three steps: First, we reconstructed the 3-D location and orientation of the joint axes of rotation from the reported two-dimensional (2-D) planar anatomical projections of the joint axes [2], [3]. Second, we converted these 3-D parametric representations into standard ("original") D-H notation [5], [6]. Third, we used Monte Carlo simulations to determine the statistical distributions of D-H parameters that result naturally from the reported anatomical variability and measurement uncertainty in the kinematic model parameters. The CMC FE axis is located in the trapezium, which is treated as the fixed base of the thumb, as is typically done in thumb models [7], [8]. The CMC AA axis is located in the proximal head of the first metacarpal while the MCP FE and AA axes are both located in the distal head of the first metacarpal. The IP FE axis is located in the distal head of the proximal phalanx (Fig. 1). The location and orientation of these instantaneous axes of rotation are assumed to be fixed with respect to the bones of the thumb [2], [3]. Thus, even as thumb configuration changes, the axes of rotation remain fixed relative to the bones of the thumb.

A. Reconstructing the 3-D Location and Orientation of the Axes From the 2-D Planar Projections

We reconstructed 3-D parametric representations of the joint axes of rotation from 2-D planar projections reported as translations (via normalized fractions of bone lengths) and rotations (via angles with respect to anatomical lines) within each bone [2], [3]. We expressed the 3-D location and orientation of each joint axis using three translational parameters (D_x, D_y, D_z) and two rotational parameters (β, γ), respectively. We defined a global Cartesian coordinate system whose origin is centered at the proximal base of the trapezium, with axes oriented as follows: $+\mathrm{x} = \mathrm{palmar}$, $+\mathrm{y} = \mathrm{radial}$, $+\mathrm{z} = \mathrm{distal}$ (Fig. 1). Using basic geometric principles relating vectors in 3-D space to their 2-D projections onto planes, we calculated the 4×4 coordinate transformation matrix T that maps a frame coincident with the global coordinate system into each axis of rotation reference frame by 1) rotating about the global z axis by the angle β, 2) rotating about the local y axis by the angle $-\gamma$, and 3) translating with respect to the global coordinate system by the vector $\underline{D} = \{D_x, D_y, D_z\}$ [9]. This transformation (Fig. 2) mapped the global x axis into the reported axis of rotation

$$T = \begin{bmatrix} 1 & 0 & 0 & D_x \\ 0 & 1 & 0 & D_y \\ 0 & 0 & 1 & D_z \\ 0 & 0 & 0 & 1 \end{bmatrix} * \begin{bmatrix} \cos\beta & -\sin\beta & 0 & 0 \\ \sin\beta & \cos\beta & 0 & 0 \\ 0 & 0 & 1 & 0 \\ 0 & 0 & 0 & 1 \end{bmatrix}$$
$$* \begin{bmatrix} \cos(-\gamma) & 0 & \sin(-\gamma) & 0 \\ 0 & 1 & 0 & 0 \\ -\sin(-\gamma) & 0 & \cos(-\gamma) & 0 \\ 0 & 0 & 0 & 1 \end{bmatrix}. \quad (1)$$

B. Converting 3-D Parametric Representations of the Axes Into Denavit-Hartenberg Notation

The standard ("original") D-H notation [5], [6] is a well-established method for expressing the relationship between two

successive DOFs (prismatic or revolute) in a serial chain. We chose this notation, as opposed to the "modified" D-H notation (as in [10]), because it is well-accepted in the robotics field and serves as a standardized way of sharing kinematic models among researchers. According to convention, we defined each axis of rotation as a "z axis" about which the next distal link rotates (i.e., a revolute DOF for roboticists). To transform from one DOF z_{n-1} to the next distal DOF z_n via their common normal x_n (which points toward z_n), one simply needs four D-H parameters (θ, d, a, α). These parameters specify 1) rotation of x_{n-1} about z_{n-1} by θ_n, 2) translation along z_{n-1} by d_n, 3) translation along x_{n-1} by a_n, and 4) rotation of z_{n-1} about x_n by α_n. By convention, the DOF joint variable is θ for revolute joints and d for prismatic joints. For the five-hinge model we used, all five DOF variables were joint rotation angles θ_n. We determined baseline θ_n values corresponding to a reference configuration of the thumb, in which the bones are longitudinally aligned (Fig. 1). Angular changes (positive for flexion and adduction) added to these baseline θ_n values specify other thumb postures.

The global coordinate system z axis was labeled z_0, and the CMC FE axis, the most proximal DOF, was appropriately labeled z_1. The labeling continued distally up to the IP FE or z_5 axis, the most distal DOF. An extra fixed transformation via a frozen "dummy" DOF (z_6) was added, as is customary in robotics [9], to define the thumbtip reference frame (z_7) (Fig. 1). We defined the origin of the z_6 frame to be coincident with the origin of the z_5 frame. We defined the thumbtip z_7 frame, fixed and centered at the distal end of the distal phalanx, to be aligned with the global x, y, and z axes when the thumb is in the reference configuration (Fig. 1).

Per D-H conventions, each common normal x_n pointed away from z_{n-1} toward z_n. Cross-products determined the common normal direction x_n for each successive pair of z axes

$$\vec{x}_n = \frac{(\vec{z}_{n-1} \times \vec{z}_n)}{\|\vec{z}_{n-1} \times \vec{z}_n\|} \quad (2)$$

and the minimum distance between the skew lines z_n and z_{n-1} determined the length of each common normal a_n

$$a_n = abs\left(\frac{\vec{w} \cdot \vec{x}_n}{\|\vec{x}_n\|}\right) \quad (3)$$

where the vector w connects a point on z_{n-1} to a point on z_n.

To calculate the distance d_n on a z axis (z_{n-1}) between its successive common normals (x_{n-1}, x_n), we need the points of intersection between each z axis and its successive common normals. We used parametric equations to represent points $\{a, b, c\}$ and $\{d, e, f\}$ on z_{n-1} and z_n, respectively

$$\{a, b, c\} = \{x_{z_{n-1}}, y_{z_{n-1}}, z_{z_{n-1}}\} + t_{n-1}(\vec{z}_{n-1}) \quad (4)$$
$$\{d, e, f\} = \{x_{z_n}, y_{z_n}, z_{z_n}\} + t_n(\vec{z}_n). \quad (5)$$

We calculated the parameters t_{n-1} and t_n by simultaneously solving the following equations:

$$a_n = \sqrt{(a - d)^2 + (b - e)^2 + (c - f)^2} \quad (6)$$
$$0 = [(a - d), (b - e), (c - f)] \cdot \vec{z}_n. \quad (7)$$

We used the facts that the distance between the two points must be equal to a_n (6) and that the vector connecting the two points must be perpendicular to the vector z_n (7).
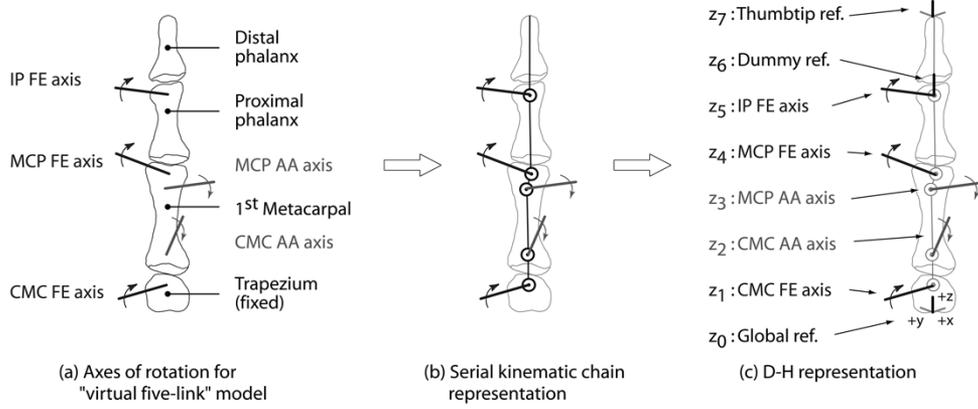
Fig. 1. (a) The anatomy-based "virtual five-link model" [4] features nonorthogonal, nonintersecting axes of rotation at the CMC and MCP joints. The dorsal aspect of a right thumb is shown. Positive rotation directions indicate flexion or adduction. (CMC = $\mathrm{carpometacarpal}$, MCP = $\mathrm{metacarpophalangeal}$, IP = $\mathrm{interphalangeal}$, FE = $\mathrm{flexion\text{-}extension}$, AA = $\mathrm{adduction\text{-}abduction}$). (b) Assuming a serial chain of five generic hinges, five "virtual" links result from the nonorthogonal and nonintersecting axes of rotation [4]. (c) A representative Type 1 kinematic model of the thumb, in which the MCP FE axis is distal to the MCP AA axis, is shown in the reference configuration with z axes noted according to D-H convention. The D-H parameters and bone dimensions for this representative sample are presented in Tables III and IV, respectively.
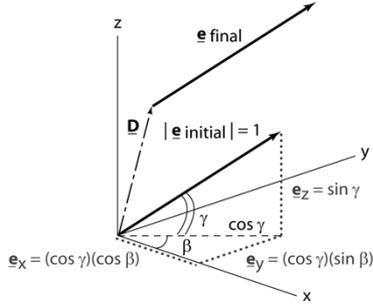
Fig. 2. Conversion of the anatomy-based joint axis vectors to our parametric representation (angles β and γ, and vector $\underline{D}$). The 3-D orientation of each joint axis of rotation (represented by unit vector $\underline{e}_{initial}$) with respect to each bone of the thumb was obtained from the literature [2], [3]. We then projected $\underline{e}_{initial}$ onto the x, y, and z axes and expressed the projected lengths as functions of rotational parameters β and γ. We translated $\underline{e}_{initial}$ with respect to the global coordinate system by the vector $\underline{D}$ to locate $\underline{e}_{final}$.

Once we determined t_{n-1} and t_n, we calculated the x_n-z_{n-1} and $x_n - z_n$ intersection points (4), (5). Finally, we found distances (d_n) on the z axes between successive common normals

$$d_n = \|\{\vec{z}_{n-1} \cap \vec{x}_{n-1}\} - \{\vec{z}_{n-1} \cap \vec{x}_n\}\|. \tag{8}$$

We calculated the remaining D-H parameters, θ_n and α_n, using dot products

$$\theta_n = \cos^{-1}\left(\frac{\vec{x}_{n-1} \cdot \vec{x}_n}{(\|\vec{x}_{n-1}\|)(\|\vec{x}_n\|)}\right) \tag{9}$$

$$\alpha_n = \cos^{-1}\left(\frac{\vec{z}_{n-1} \cdot \vec{z}_n}{(\|\vec{z}_{n-1}\|)(\|\vec{z}_n\|)}\right). \tag{10}$$

The angle of rotation about z_{n-1} that aligned x_{n-1} and x_n was labeled θ_n. The angle of rotation about x_n that aligned z_{n-1} and z_n was labeled α_n.

C. Performing Monte Carlo Simulations of Thumb Kinematic Models

We explored the consequences of reported anatomical variability of the thumb axes of rotation [2], [3] on D-H parameters using a well-established stochastic analysis technique: Monte Carlo simulations [1], [11], [12]. This technique is based on

the Bayesian approach in which model parameters are variables that are best described as randomly drawn values from statistical distributions (called *prior distributions*) rather than as specific constant values [13]. Considering our interest in the natural consequences of reported anatomical variability on the D-H parameters, the Monte Carlo approach is particularly well-suited for explicitly incorporating this reported anatomical variability into the kinematic model. We performed the simulations in MATLAB© (v. 6.5) on an IBM Thinkpad (1.07 GHz Intel® Celeron™).

At each Monte Carlo iteration, we randomly drew 28 anatomical parameters (12 bone dimensions, 16 parameters describing the 2-D projections of each DOF [2], [3]) (Table I) from prior distributions, our informed choice of the range and distribution of the input (anatomical) parameters. We required the distal phalanx to be shorter than the proximal phalanx, which in turn had to be shorter than the first metacarpal, and then transformed the 2-D projections into 3-D parametric representations and D-H parameters. In contrast to data-rich studies that can identify a particular prior distribution (e.g., Gaussian), sparse data sets such as ours [2], [3] should be conservatively approximated as unbiased prior distributions: uniform distributions bounded by the reported mean ± one standard deviation [1]–[3], where unknown parameter covariances are best not included to prevent artifactual distortions [1]. That is, each parameter was treated as independent and identically distributed, each drawn from a uniform distribution whose bounds were constructed using anatomical knowledge. Monte Carlo iterations were repeated until the population statistics of the ensemble of D-H parameters converged and distributions of the output (D-H) parameters stabilized. Convergence was declared when the running mean and coefficient of variance values of the output distributions changed by less than 1% for at least the last 20% of the simulations for all D-H parameters [1].

We specified the bounding-box dimensions of each thumb bone with a parallelepiped to apply the reported normalized fractions of bone lengths [2], [3] as translations. We measured the bounding-box dimensions for the trapezium, first metacarpal, proximal phalanx, and distal phalanx in eleven

TABLE I

FOR EACH MONTE CARLO SIMULATION, ANATOMICAL PARAMETERS WERE SAMPLED FROM UNIFORM PRIOR DISTRIBUTIONS BOUNDED BY THE REPORTED $\mathrm{Mean} \pm \mathrm{Standard\ Deviation}$

Bone segment lengths (cm)
(Trapezium distal length from measurements of cadaveric thumbs (n=11);
1st metacarpal, proximal phalanx, distal phalanx distal lengths from [1])

	Direction	Mean	Standard dev.
Trapezium	distal	1.36	0.28
1st metacarpal	distal	5.29	0.90
Proximal phalanx	distal	4.03	0.62
Distal phalanx	distal	3.07	0.31

Bone ratios (relative to segment distal lengths)
(Bone ratios from measurements of cadaveric thumbs (n=11))
Bone segment distal lengths were chosen and scaled by the bone ratio value.

	Direction	Mean	Standard dev.
Trapezium	palmar	1.11	0.35
	radial	1.40	0.29
1st metacarpal	palmar	0.34	0.03
	radial	0.35	0.02
Proximal phalanx	palmar	0.37	0.05
	radial	0.47	0.04
Distal phalanx	palmar	0.40	0.07
	radial	0.62	0.07

Published axis of rotation parameters [2], [3] (angles in degrees)

	Parameter	Mean	Standard dev.
CMC FE	β	13.6	16.5
	b/B	0.36	0.136
CMC AA	α	83.6	14.2
	β	78.3	12.9
	t/T	0.595	0.143
	l/L	0.125	0.062
MCP FE	α	101.0	6.0
	t/T	0.57	0.17
	l/L	0.87	0.05
MCP AA	α	80.0	9.0
	β	74.0	8.0
	t/T	0.45	0.08
	l/L	0.83	0.13
IP FE	β	83.0	4.0
	t/T	0.44	0.17
	l/L	0.90	0.05

cadaveric thumbs (7 female, 2 male (left and right thumbs from 2 female subjects); 8 left, 3 right (all female); 79 ± 6.5 years (mean $\pm$ standard deviation); dial caliper measurement accuracy of 0.1 mm). We measured these multiple dimensions ourselves because the literature only contains length ratios among the metacarpals and phalanges [14] that do not include the trapezium.

D. Finding Statistically Significant Clusters of Denavit-Hartenberg Parameters

We used cluster analysis, a data classification method [15], as implemented by MATLAB©'s "Statistical Toolbox" [16], to test whether our resulting D-H parameter distributions were multimodal. This hierarchical method uses an *agglomerative* technique in which all objects (individual simulated thumb D-H models) are initially assumed separate and get grouped together based on a *similarity metric* [15]. First, we converted the D-H angles θ_n and α_n to the $\pm180°$ range to minimize artifactual differences among clusters due to the cyclic nature of angles. Then we created a matrix of objects where rows corresponded to individual models and columns corresponded to D-H parameter values. Using MATLAB©'s "pdist" command and "seuclidean" option, we calculated our similarity metric: standardized Euclidean distance between each possible pair of objects (rows). Standardized Euclidean distance is calculated similarly

to Euclidean distance except that each column variable (separate D-H parameter) in the sum of squares is divided by the sample variance of that coordinate. Thus, differences between clusters were independent of differences in measurement units (meters for lengths a_n and d_n, degrees for angles θ_n and α_n). Using MATLAB©'s "linkage" command and "average" option, we created hierarchical clusters based on the average standardized Euclidean distance between all pairs of objects in each cluster. The grouping continued automatically until all objects had been clustered into one large group and the clustering order had been determined. Using MATLAB©'s "dendrogram" command, we specified the number of clusters we wanted to analyze pictorially. We manually increased the number of clusters from one until we eliminated all visually obvious bimodal clusters as observed in a histogram postanalysis. We preliminarily deemed each cluster a separate type of kinematic model and used one-way analysis of variance and Scheffé's *post hoc* procedure [17] ($\alpha = 0.05$) to determine the statistical significance of the differences between clusters.

E. Characterizing the Statistical Distributions of the D-H Parameters

We characterized each D-H parameter distribution for each cluster using standard parametric, continuous statistical distributions, such as the beta (A, B), gamma (shape ϕ, scale λ), normal (μ, σ), and a mixture of two univariate normal densities $(\pi_i, \mu_i, \sigma_i$ for $i = 1, 2)$ [13], [18]. To estimate the distribution parameters, we used a penalized expectation-maximization algorithm for the normal mixture case [18] and standard MATLAB© maximum-likelihood estimate functions for the others.

Once we estimated distribution parameters, we checked for goodness of fit between the theoretical distributions and the empirically based histograms from the Monte Carlo simulations, and reported those with the best fit. We used the two-stage δ-corrected Kolmogorov-Smirnov test [19] ($\alpha = 0.05$) to check for goodness of fit of the normal distribution. This test is based on differences between the hypothesized theoretical cumulative distribution function and the empirical cumulative distribution function, which depends critically on the manner in which the histogram is divided, or "binned." To set the bin size in the histograms appropriately, we used the default "Sturges" bin-selection algorithm, readily available in the statistical computing environment of *R* (v. 1.6.1) [20]. The Kolmogorov–Smirnov test is known to have more power than the standard χ^2 goodness of fit test and is more robust to arbitrary bin-size selection in histograms. Empirical statistical tables which have been developed specifically for the two-stage δ-corrected Kolmogorov–Smirnov test of normality [21], assuming maximum-likelihood estimates estimated from the data itself, are not yet available for the other statistical distributions we considered [22]. As a result, we used the standard χ^2-test ($\alpha = 0.05$) to test for goodness of fit of the theoretical beta, gamma, and normal mixture distributions.

III. RESULTS

We successfully translated the five DOFs of the thumb from the reported 2-D anatomical projections into D-H notation as evidenced by convergence of the Monte Carlo simulations after

TABLE II

DISTRIBUTIONS FOR THE FOUR TYPES OF D-H PARAMETER SETS (θ AND α IN DEGREES, d AND a IN CENTIMETERS) ARE PRESENTED USING THE FOLLOWING NOTATION: **BETA** $B(A, B)$, **GAMMA** $G(\text{shape } \phi, \text{ scale } \lambda)$, **NORMAL** $N(\mu, \sigma)$, AND A **MIXTURE OF TWO UNIVARIATE NORMAL DENSITIES** $NM(\pi_1, \mu_1, \sigma_1; \pi_2, \mu_2, \sigma_2)$. PARAMETER DISTRIBUTIONS THAT FAILED THE χ^2-TEST FOR GOODNESS OF FIT WERE CHARACTERIZED BY THE DISTRIBUTION THAT MOST CLOSELY MATCHED (INDICATED BY A §). BOUNDARY VALUES FOR THEORETICALLY UNBOUNDED PARAMETER DISTRIBUTIONS (GAMMA, NORMAL, MIXTURE OF TWO UNIVARIATE NORMAL DENSITIES) ARE REPORTED AS [LOWER BOUND, UPPER BOUND]. THE DISTRIBUTION FOR EACH θ_5 CLUSTER (FIG. 3) IS INDICATED BY A BOLD BOX. POSITIVE ANGLES OF FLEXION OR ADDUCTION CAN BE ADDED TO THE θ VALUES TO SPECIFY THUMB POSTURES AWAY FROM THE REFERENCE CONFIGURATION (FIG. 1). BONE DIMENSION DISTRIBUTIONS THAT CORRESPOND WITH THESE D-H PARAMETER DISTRIBUTIONS ARE THE **UNIFORM** $U(\mu - \sigma, \mu + \sigma)$ DISTRIBUTIONS BOUNDED BY THE "BONE SEGMENT LENGTH" AND "BONE RATIO" VALUES FROM TABLE I

Type 1

	θ	d	a	α
z_6 to z_7	0	N (3.47, 0.22); [2.91, 4.09]	B§ (2.60, 1.57) × 0.60 - 0.40	0
z_5 to z_6	180	NM§ (0.47, -17.39, 4.11; 0.53, -11.91, 1.73); [-31.93, -6.07]	0	B (0.94, 0.88) × 8.00 + 93.00
z_4 to z_5	B§ (1.65, 1.77) × 22.55 - 107.90	G§ (3.04, 0.44) + 7.74; [6.08, 31.92]	B (1.09, 2.15) × 0.61	B (2.09, 2.17) × 19.66 + 8.30
z_3 to z_4	N (-20.80, 19.06); [-69.72, 39.72]	B§ (9.17, 6.33) × 17.57 - 13.30	B (1.37, 2.07) × 1.22 + 0.01	B§ (1.52, 1.54) × 17.96 + 98.25
z_2 to z_3	NM (0.21, 19.67, 11.43; 0.79, 51.52, 16.32); [-9.69, 99.69]	NM§ (0.70, 3.00, 1.75; 0.30, 4.25, 2.93); [-5.92, 13.92]	N (2.92, 0.68); [0.52, 4.98]	NM (0.73, -36.92, 6.53; 0.27, -23.79, 5.24); [-59.68, -10.32]
z_1 to z_2	B§ (1.92, 1.67) × 34.62 - 117.39	N§ (-0.21, 0.27); [-1.00, 0.50]	N (1.26, 0.22); [0.61, 1.99]	B (1.95, 1.59) × 32.79 - 98.37
z_0 to z_1	0	B (0.97, 0.95) × 0.28 + 0.54	B§ (2.43, 1.23) × 0.61 - 0.61	B (0.98, 0.96) × 32.96 - 120.07

Type 4

	θ	d	a	α
z_6 to z_7	0	B (2.56, 2.89) × 1.08 + 2.96	B§ (1.90, 2.19) × 0.57 - 0.43	0
z_5 to z_6	0	NM§ (0.38, -17.88, 4.19; 0.62, -12.53, 2.12); [-33.91, -6.09]	0	B§ (1.01, 1.07) × 7.99 + 93.01
z_4 to z_5	B§ (1.83, 2.12) × 23.89 + 72.06	G (2.79, 0.42) + 8.02; [8.03, 33.97]	B (1.07, 2.19) × 0.53	B (2.09, 2.04) × 18.87 - 27.39
z_3 to z_4	N (-19.78, 18.63); [-79.34, 49.34]	NM§ (0.32, -3.97, 2.92; 0.68, -2.55, 1.40); [-11.90, 7.90]	B (1.32, 2.21) × 1.23	B§ (1.51, 1.61) × 18.27 + 98.26
z_2 to z_3	N (44.74, 20.03); [-29.57, 99.57]	NM§ (0.70, 2.88, 1.67; 0.30, 4.12, 3.00); [-7.90, 11.90]	N§ (2.91, 0.65); [0.52, 4.98]	N (-33.43, 8.65); [-59.65, -5.35]
z_1 to z_2	B§ (1.77, 1.66) × 34.80 - 116.91	N (-0.22, 0.28); [-1.00, 0.60]	B§ (2.94, 3.32) × 1.20 + 0.70	B§ (2.22, 1.70) × 34.29 - 99.46
z_0 to z_1	0	B§ (1.02, 1.04) × 0.28 + 0.54	B§ (2.05, 1.20) × 0.55 - 0.55	B§ (0.99, 1.02) × 32.92 - 120.06

Type 2

	θ	d	a	α
z_6 to z_7	0	N (3.47, 0.22); [3.01, 4.00]	N (-0.09, 0.15); [-0.40, 0.20]	0
z_5 to z_6	B (0.97, 1.55) × 17.10 + 69.40	N (-0.90, 0.21); [-1.40, -0.50]	0	N (97.04, 2.19); [93.01, 100.99]
z_4 to z_5	N (160.50, 4.48); [152.04, 171.96]	N (-1.24, 0.43); [-2.19, -0.21]	N (4.16, 0.34); [3.40, 4.80]	N (104.14, 4.10); [94.07, 111.93]
z_3 to z_4	N (193.34, 11.17); [170.12, 214.88]	N (0.56, 0.34); [-0.59, 1.59]	B (1.18, 4.95) × 0.15	N (107.82, 4.14); [98.19, 117.81]
z_2 to z_3	N (25.18, 10.38); [5.09, 44.91]	N (0.99, 0.82); [-0.97, 2.47]	N (3.81, 0.49); [2.81, 4.99]	N (77.10, 6.78); [60.58, 94.42]
z_1 to z_2	N (-99.71, 8.72); [-114.71, -80.29]	N (-0.21, 0.32); [-0.98, 0.58]	N (1.30, 0.20); [0.80, 1.80]	N (-80.38, 6.78); [-99.70, -65.30]
z_0 to z_1	0	N (0.68, 0.08); [0.51, 0.84]	B (1.43, 1.16) × 0.39 - 0.40	N (-102.96, 10.31); [-124.55, -85.45]

Type 3

	θ	d	a	α
z_6 to z_7	0	N (3.47, 0.21); [2.91, 4.00]	B (1.93, 1.56) × 0.61 - 0.42	0
z_5 to z_6	B§ (1.62, 1.46) × 20.22 + 67.81	N (-0.78, 0.23); [-1.60, -0.20]	0	B (1.01, 0.96) × 8.00 + 93.00
z_4 to z_5	B (2.38, 2.16) × 20.61 - 29.13	N (-0.90, 0.45); [-2.39, 0.39]	B (2.73, 3.20) × 1.99 + 3.03	B§ (1.76, 1.60) × 18.91 + 94.68
z_3 to z_4	B (3.03, 2.90) × 52.56 - 16.64	B§ (4.65, 5.34) × 2.46 - 0.57	B§ (1.15, 2.63) × 0.79	B§ (1.55, 1.55) × 18.13 - 116.36
z_2 to z_3	B (1.92, 2.13) × 45.38 + 2.64	NM§ (0.48, 0.14, 0.44; 0.52, 1.35, 0.51); [-1.48, 2.98]	NM (0.39, 3.45, 0.28; 0.61, 4.03, 0.37); [2.80, 5.20]	B§ (1.56, 1.79) × 29.72 + 63.42
z_1 to z_2	B (2.09, 1.88) × 35.48 - 117.08	N (-0.20, 0.27); [-1.00, 0.50]	NM§ (0.55, 1.12, 0.16; 0.45, 1.42, 0.17); [0.61, 1.90]	B§ (2.48, 1.92) × 35.05 - 99.60
z_0 to z_1	0	B§ (1.07, 1.10) × 0.28 + 0.54	B§ (2.55, 1.25) × 0.62 - 0.62	B§ (1.05, 1.00) × 32.95 - 120.08

3550 simulations. The D-H parameter θ_3, a rotational parameter relating the second DOF to the third DOF in the serial chain model, took the longest to converge. Mean and coefficient of variance for θ_3 changed by less than 1% for the remainder of the simulations after 1390 and 2839 simulations, respectively, necessitating an additional 711 simulations to satisfy the convergence criteria for a total of 3550 simulations.

A multimodal distribution is apparent from visual inspection of the 3550 D-H parameter sets, particularly for θ_5 (a rotational parameter relating the fourth DOF to the fifth DOF in the serial chain model, Fig. 3), which cluster analysis grouped into four statistically significant types of thumb kinematic models (Fig. 3; $p < 0.0001$), as confirmed by one-way analysis of variance. Scheffé's *post hoc* procedure determined that all possible pairwise comparisons between the four types were statistically significant at the $\alpha = 0.05$ level.

Table II shows the D-H parameter distributions for the four types of models. These D-H parameters describe the details of
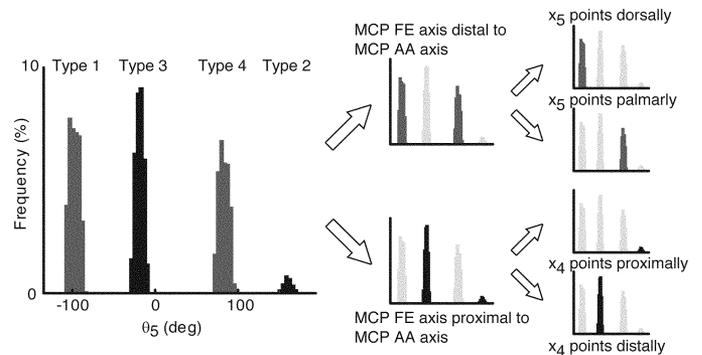
Fig. 3. Cluster analysis of the 3550 D-H parameter sets confirmed their grouping into four types. One-way analysis of variance and Scheffé's *post hoc* procedure confirmed that the four groups were statistically significant at the $\alpha = 0.05$ level. The multimodal nature of rotational D-H parameter θ_5 data is shown.

the transformations to go from the global coordinate system, z_0, to axes of rotation z_1 through z_5, dummy axis z_6, and thumbtip

TABLE III
REPRESENTATIVE VALUES FOR THE FOUR TYPES OF D-H PARAMETER SETS (θ AND α IN DEGREES, d AND a IN CENTIMETERS) ARE PRESENTED FOR DIRECT IMPLEMENTATION IN A ROBOTICS-BASED THUMB MODEL. WE REPORT THE MEDIAN FOR EACH θ_5 CLUSTER (FIG. 3), INDICATED BY A BOLD BOX, AND THE VALUES OF THE REMAINING D-H PARAMETERS DRAWN DURING THAT PARTICULAR SIMULATION. POSITIVE ANGLES OF FLEXION OR ADDUCTION CAN BE ADDED TO THE θ VALUES TO SPECIFY THUMB POSTURES AWAY FROM THE REFERENCE CONFIGURATION (FIG. 1)

	Type 1 θ	Type 1 d	Type 1 a	Type 1 α	Type 4 θ	Type 4 d	Type 4 a	Type 4 α
z_6 to z_7	0	3.81	0.01	0	0	3.29	-0.13	0
z_5 to z_6	180	-17.32	0	97.07	0	-12.14	0	95.91
z_4 to z_5	**-97.10**	17.13	0.08	12.75	**82.95**	12.59	0.10	-21.63
z_3 to z_4	-32.03	-3.06	0.39	99.20	1.94	-1.89	1.03	100.93
z_2 to z_3	66.02	4.01	2.72	-39.61	28.89	1.54	3.56	-29.92
z_1 to z_2	-114.92	-0.67	1.13	-76.60	-92.57	-0.10	1.51	-69.59
z_0 to z_1	0	0.77	-0.11	-115.49	0	0.68	-0.10	-103.37

	Type 2 θ	Type 2 d	Type 2 a	Type 2 α	Type 3 θ	Type 3 d	Type 3 a	Type 3 α
z_6 to z_7	0	3.64	-0.18	0	0	3.42	0.03	0
z_5 to z_6	70.20	-1.11	0	98.35	74.47	-0.71	0	94.89
z_4 to z_5	**160.35**	-1.82	4.35	106.14	**-18.41**	-1.16	3.99	106.43
z_3 to z_4	200.70	0.10	0.05	111.73	4.08	0.85	0.31	-110.37
z_2 to z_3	23.07	1.61	3.22	70.77	16.81	-0.51	4.45	88.41
z_1 to z_2	-104.22	-0.35	1.47	-75.03	-85.11	0.21	1.31	-86.86
z_0 to z_1	0	0.80	-0.38	-101.41	0	0.59	-0.12	-93.86

TABLE IV
BOUNDING-BOX BONE DIMENSIONS (IN CENTIMETERS) ARE PRESENTED FOR MODELS WHOSE REPRESENTATIVE D-H PARAMETER VALUES ARE REPORTED IN TABLE III

	Type 1 Palmar (x)	Type 1 Radial (y)	Type 1 Distal (z)	Type 4 Palmar (x)	Type 4 Radial (y)	Type 4 Distal (z)
Distal phalanx	1.35	1.87	3.34	1.26	1.83	2.84
Proximal phalanx	1.47	1.67	3.74	1.76	2.19	4.62
1st Metacarpal	1.76	1.72	5.06	2.11	2.11	5.98
Trapezium	2.23	2.43	1.53	1.19	1.59	1.35

	Type 2 Palmar (x)	Type 2 Radial (y)	Type 2 Distal (z)	Type 3 Palmar (x)	Type 3 Radial (y)	Type 3 Distal (z)
Distal phalanx	1.45	2.07	3.30	1.24	1.71	2.86
Proximal phalanx	1.50	2.11	4.15	1.52	2.02	4.46
1st Metacarpal	1.73	1.68	4.98	1.94	1.96	5.80
Trapezium	1.40	2.19	1.59	0.98	1.56	1.18
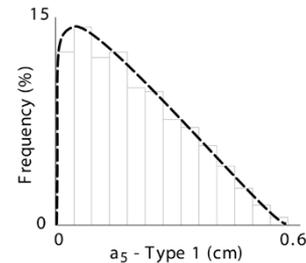
Fig. 4. The statistical distribution of translational D-H parameter a_5 data for Type 1 was characterized by a beta $B(1.09, 2.15)$ distribution scaled by 0.61. The χ^2 test resulted in a p-value of 0.71, indicating that there was insufficient evidence ($\alpha = 0.05$) to reject the hypothesized beta distribution.

reference axis z_7. Tables III and IV show representative D-H parameter and bone-dimension values, respectively, from one kinematic model of each type because descriptive statistics (e.g., mean) for skewed D-H parameter distributions (Fig. 4) may not be representative of the relationships among the axes of rotation for any one Monte Carlo simulation.

A biomechanically distinct kinematic feature differentiated the four types of kinematic models (Fig. 3): the order of FE and AA axes of rotation at the MCP joint. In 65.2% of all models (Types 1, 4), the MCP FE axis was distal to the MCP AA axis (Fig. 1). A detail of D-H notation further subdivided these two groups by specifying the direction of the common normals associated with DOFs z_4 and z_5. Specifically, common normal x_5 pointed dorsally in Type 1 (36.0%) and palmarly in Type 4 (29.2%). Common normal x_4 pointed proximally in Type 2 (2.2%) and distally in Type 3 (32.6%).

IV. DISCUSSION

In this study that establishes the effects of anatomical variability on a kinematic structure of the thumb with hinged linkages, we: 1) translated an anatomy-based kinematic model of the thumb into a standard robotics notation (D-H); and 2) used Monte Carlo simulations to converge on the statistical distributions of D-H parameters that naturally emerge from the re-

ported variability in that anatomical kinematic model. Cluster analysis and one-way analysis of variance of the 3550 D-H parameter sets confirmed their grouping into four distinct types of thumb kinematic models. The order of FE and AA axes at the MCP joint was the main distinguishing feature among types of kinematic models. Our conversion into D-H notation serves two purposes. First, it characterizes the distributions of D-H parameters that emerge directly from the reported anatomical variability [2], [3]. Second, it provides representative D-H parameter sets that can be easily incorporated into robotics-based musculoskeletal models of the thumb.

A. Rationale for Using the Denavit-Hartenberg Description of Joint Kinematic Structure

Our previous work has shown that universal joints (with orthogonal and intersecting axes of rotation, by definition) at the CMC and MCP joints are unable to reproduce static thumbtip force production [1]. Universal joints are a subset of the general case where consecutive axes of rotation are at an arbitrary distance and orientation from one another, which is effectively described using D-H notation. Note that we assume, based on cadaveric studies [2]–[4], that the kinematic structure of the thumb

is a serial chain with five, invariant, nonorthogonal and nonintersecting rotational DOFs. This study is a necessary step toward our overall goal of establishing whether it is possible to create realistic musculoskeletal thumb models using a robotics-based approach that approximates thumb kinematic structure with hinged linkages (i.e., fixed-length serial linkages articulated only by rotational DOFs).

The "virtual five-link" model of the thumb [4] provides anatomical evidence for nonorthogonal and nonintersecting axes of rotation in the kinematic structure of the thumb. Using this anatomy-based "virtual five-link" kinematic structure in musculoskeletal thumb models necessitates translating anatomical descriptions of axes of rotation into standard robotics notation. We chose the standard ("original") D-H parameter notation because it is a well-accepted notation in the robotics field, allows for standardized sharing of kinematic models among researchers, and any subtle deviations from this convention are a matter of preference. We are aware that the human hand has been modeled using a combination of robotics notation, namely D-H notation for nearly perpendicular successive axes and the Hayati convention for nearly parallel successive axes [23]. However, this use of dual notation was applied to a model that assumed orthogonal and intersecting axes of rotation as well as perfectly parallel successive axes of rotation. In the "virtual five-link" model we consider, adjacent hinges of the serial chain model are nonintersecting, nonorthogonal, and nonparallel. Furthermore, as will be discussed later, the proximal-to-distal sequence of the hinges can change, which would necessitate the use of different combinations of robotics notation at each Monte Carlo simulation. It is important to note that the overall kinematic *model structure* [24] does not change, but the manner in which the structure can be expressed (equivalently D-H, Hayati, or a combination of both) can change. For general applicability and consistency with the work of roboticists, we adopted the D-H notation.

B. Advantages and Limitations of the Monte Carlo Method as Applied to Biomechanical Models

Monte Carlo simulations are an effective means to characterize the distribution of D-H parameters for the thumb given variability in anatomical parameters. More generally speaking, the Monte Carlo method is a Bayesian approach to build distributions of output (e.g., D-H) parameters by repeatedly, randomly drawing from prior distributions of input (e.g., anatomical) parameters informed by our knowledge of anatomical ranges, variability, and uncertainty of parameter measurements. Each Monte Carlo simulation performed the conversion of a set of anatomical parameters into D-H parameters. The D-H parameter distributions we report (Table II) are well-informed because they result directly from the reported anatomical variability of the thumb [2], [3].

As a valid first step, we treated each parameter as independent and identically distributed, each drawn from a uniform prior distribution whose bounds were constructed using anatomical knowledge. It should be noted that the details of the prior distributions (Table I) and any covariance among them necessarily affect the resulting output distributions (Table II). We assume independence among anatomical parameters (bone dimensions, parameters describing the 2-D projection of each DOF) because

there are no reports of covariance among thumb parameters (e.g., among and across bone lengths) to our knowledge [1]. The limitation of this conservative approach is that it *may* broaden the output distributions by simulating a wider variety of thumbs than are likely to exist in reality—but assuming arbitrary covariances would *certainly* affect the output distributions in artifactual and possibly misleading ways [1]. We do use as few anatomical parameters as possible in our model, and use relative bone proportion measurements from cadaveric thumbs to guide the uniform distribution boundaries for the depth and width bone dimensions used to build the bounding-boxes. Nonetheless, even these proportion values were allowed to vary about the mean by one standard deviation and so strict covariances were not applied. Our current work in cadaveric thumbs [25] will allow us to build a database of bone lengths that, in the future, will allow us to set covariances among bone lengths to reduce the number of model parameters.

C. Identification of Distinct Types of Thumb Kinematic Models

A multimodal distribution is apparent from visual inspection of the 3550 D-H parameter sets, particularly for θ_5 (Fig. 3). This rotational parameter relates the fourth DOF to the fifth DOF in the serial chain model and depends on the relative orientation of the DOFs it relates. For instance, θ_5 will take on different values when relating two nearly parallel axes (e.g., MCP FE and IP FE axes) as opposed to two nearly orthogonal axes (e.g., MCP AA and IP FE axes). Although θ_n parameters are rotational DOFs used to vary posture, and are, therefore, not "fixed," our identification of distinct types of kinematic models based on θ_n values is valid, as we used baseline values that corresponded to a reference thumb configuration (Fig. 1) across all models. These baseline θ_n values are unique to each model and are not artifacts of the posture of the cadaveric specimens at the time of measurement. This is because the cadaveric specimens were passively moved throughout their range of motion, through numerous postures, to establish the "virtual five-link" kinematic model whose instantaneous axes of rotation are assumed to be fixed with respect to the bones of the thumb [2], [3].

Cluster analysis of the D-H parameter distributions confirmed four types of thumb kinematic models differentiated primarily by axis of rotation order at the MCP joint, and further subdivided by a detail of D-H notation specifying the direction of the common normals associated with DOFs z_4 and z_5. We believe this latter detail is of little biomechanical significance because it is a reflection of one DOF pointing slightly above or below, for example, the next distal DOF in the serial chain.

The fact that all models can be distinguished by the sequential order of MCP FE and AA axes is biomechanically significant because DOF order can be critical to the kinematic behavior of any serial chain model and necessarily affects biomechanical function. The MCP AA axis was described in the literature as moving with the proximal phalanx about the MCP FE axis located in the first metacarpal [3]. In the framework of the serial chain model, this necessitates that the MCP AA axis be distal to the MCP FE axis. Yet, our results show that the reported anatomical variability at the MCP joint [3] naturally leads to changes in axis order at the MCP joint. From the overlapping (mean ± standard deviation) distributions reported for the anatomical parameters associated with the MCP FE and AA

axes [3], it is unclear whether a fixed FE/AA axis order was consistently observed at the MCP joint in all cadaveric specimens reported in [3]. Interestingly, a study has reported a bimodal pattern of active thumb range of motion at the MCP joint [26] which could be related to the kinematic consequences of the two MCP joint scenarios we observed. Other thumb studies report sex-based differences in bone geometry and joint congruity at the CMC joint [27] and bone geometry and range of motion at the MCP joint [28]. However, we do not know the exact role that subject sex or hand size played in our Monte Carlo simulations, if any, because the data we use [2], [3] and results we present are inclusive of sex and hand size effects.

It is important to note that the four types of thumb kinematic models naturally emerged from variability in anatomical measurements of cadaveric specimens [2], [3], as opposed to variability in *in vivo* functional measurements. By building a strong anatomy-based kinematic foundation, we have established a finite set of kinematic model possibilities that are not confounded by the currently unknown ability/inability of the neuromuscular system to place the thumb in every kinematically possible configuration. We are currently implementing the four types of kinematic models in muscle-driven musculoskeletal models to establish their functional consequences, and compare those to results of future *in vivo* studies. After comparisons to *in vivo* functional measurements, we expect a functional subset of models to emerge from the current set of anatomy-based possibilities.

D. Application of D-H Parameters to Implement Novel Biomechanical Models of the Thumb

This work provides the D-H representation for the "virtual five-link" thumb kinematic structure [4] instrumental to implementing musculoskeletal models based on principles of robotics. Our reported statistical distributions of D-H parameters for the four types of models can be used as informed prior distributions for our continuing development of stochastic musculoskeletal thumb models [1]. The D-H parameters describe the transformations to go from the global coordinate system, z_0, to axes of rotation z_1 through z_5, dummy axis z_6, and thumbtip reference axis z_7 (Table II). In practice, one can draw a random value from an unbounded distribution (e.g., gamma, normal, normal mixture), discard the value if it is not within specified bounds (Table II), and repeat draws until the desired number of samples is obtained [11]. This ensures that values are drawn in the appropriate proportions and still reflect the bounds observed during the Monte Carlo analysis.

We also present representative parameter values from one kinematic model of each type (Table III) because descriptive statistics (e.g., mean) for skewed D-H parameter distributions (Fig. 4) may not be representative of the relationships among the axes of rotation for any one Monte Carlo simulation. Typical measures of central tendency include the mode, mean, and median [17]. To avoid reporting multiple modes (e.g., normal mixture) or measures influenced by extreme observations (e.g., mean) for each D-H parameter, we report the *median* of each θ_5 cluster (Fig. 3), and the values of the remaining D-H parameters and bone dimensions drawn during that particular simulation (Tables III and IV). These values can be directly implemented in a robotics-based model of the thumb.

These representative D-H parameter values have already been used to add human hands to the repertoire of GraspIt! [29], a visualization and simulation engine designed for the study of grasp planning in robotic hands. The D-H representation of skewed, nonintersecting, nonorthogonal axes of rotation for the thumb provides a new biomimetic direction for comparative kinematic studies of robotic and human hands, and may help elucidate whether and how these kinematic features enable dexterous manipulation in humans. There is currently a need for the implementation of such thumb kinematic models because our previous work has shown that orthogonal and intersecting axes of rotation at the CMC and MCP joints are unable to realistically predict maximal 3-D fingertip forces and the coordination patterns that produce them [1]. An anatomically realistic kinematic representation is critical to musculoskeletal models because the kinematic structure of the thumb defines the fundamental relationship between joint angles and 3-D thumb posture, and their derivatives, as well as the mapping between joint torques and thumbtip forces and torques [24]. Thus, an appropriate kinematic structure is essential to the usefulness of a thumb model to realistically predict motion and force in 3-D. More fundamentally, this work is a necessary step in determining whether thumb joints may be adequately modeled as hinges amenable for standard robotic analysis in spite of reports of load-dependent motion of the trapezium [25], [30], or if it is necessary to invest the analytical and computational effort to move toward full "contact" models where the kinematic behavior of the thumb arises from the interactions among joint contact surfaces, ligaments and loads, as in the case of the knee [24], [31], [32].

E. Generic Versus Subject-Specific Versus Modular Biomechanical Models

This work redefines the context in which to address the long-debated issue of whether a single generic biomechanical model can be representative of the population at large, or if subject-specific models are necessary for clinical applications [24]. By establishing how the natural anatomical variability affects thumb kinematic structure (described using D-H parameter distributions) we find a third alternative to the modeling debate: that the thumb kinematic structure of a population may be described by a finite number of statistically distinct model-types. Assembling an informative biomechanical model for a particular individual may be done modularly by, say, using generic CMC and IP joints, with the appropriate type of MCP joint determined via some discriminating functional test. Clearly, additional work is needed to determine those discriminating tests, but this alternative is well aligned with clinical observations of a finite number of characteristic modes of disease progression and response to treatment. The critical challenge would then be to develop predictive tests to identify the timing and selection of treatment for a specific patient [33]. If each patient could at least be categorized by a model-type that is, say, particularly susceptible to certain pathologies and particularly responsive to certain treatments, this would increase the patient's chances of successful diagnosis, treatment, and restoration of function. Exploring the possibility that multimodal thumb structure and function affect disease progression and response to treatment is critical to the generalizability and clinical usefulness of biomechanical models of the thumb. Our current and future work,

therefore, focuses on understanding the functional consequence of these types of thumb kinematic models in muscle-driven musculoskeletal models.

REFERENCES

[1] F. J. Valero-Cuevas, M. E. Johanson, and J. D. Towles, "Toward a realistic biomechanical model of the thumb: The choice of kinematic description may be more critical than the solution method or the variability/uncertainty of musculoskeletal parameters," *J. Biomech.*, vol. 36, pp. 1019–1030, Jul. 2003.

[2] A. M. Hollister, W. L. Buford, L. M. Myers, D. J. Giurintano, and A. Novick, "The axes of rotation of the thumb carpometacarpal joint," *J. Orthop. Res.*, vol. 10, pp. 454–460, May 1992.

[3] A. M. Hollister, D. J. Giurintano, W. L. Buford, L. M. Myers, and A. Novick, "The axes of rotation of the thumb interphalangeal and metacarpophalangeal joints," *Clin. Orthop. Related Res.*, vol. 320, pp. 188–193, Nov. 1995.

[4] D. J. Giurintano, A. M. Hollister, W. L. Buford, D. E. Thompson, and L. M. Myers, "A virtual five-link model of the thumb," *Med. Eng. Phys.*, vol. 17, pp. 297–303, Jun. 1995.

[5] J. Denavit and R. S. Hartenberg, "A kinematic notation for lower-pair mechanisms based on matrices," *J. App. Mech.*, vol. 22, pp. 215–221, Jun. 1955.

[6] R. P. Paul, B. Shimano, and G. E. Mayer, "Kinematic control equations for simple manipulators," *IEEE Trans. Syst., Man, Cybern.*, vol. SMC-11, no. 6, pp. 449–455, Jun. 1981.

[7] W. P. Cooney III and E. Y. Chao, "Biomechanical analysis of static forces in the thumb during hand function," *J. Bone Joint Surg. Am.*, vol. 59-A, pp. 27–36, Jan. 1977.

[8] F. Schuind, K. N. An, W. P. Cooney III, and M. Garcia-Elias, *Advances in the Biomechanics of the Hand and Wrist*. New York: Plenum, 1994.

[9] T. Yoshikawa, *Foundations of Robotics: Analysis and Control*. Cambridge, MA: MIT Press, 1990.

[10] J. J. Craig, *Introduction to Robotics: Mechanics and Control*. Reading, MA: Addison-Wesley, 1989.

[11] G. S. Fishman, *Monte Carlo: Concepts, Algorithms, and Applications*. New York: Springer, 1996.

[12] R. E. Hughes and K. N. An, "Monte carlo simulation of a planar shoulder model," *Med. Biol. Eng. Comput.*, vol. 35, pp. 544–548, Sep. 1997.

[13] J. A. Rice, *Mathematical Statistics and Data Analysis*. Belmont, CA: Duxbury, 1995.

[14] A. Aydinlioglu, F. Akpinar, and N. Tosun, "Mathematical relations between the lengths of the metacarpal bones and phalanges: Surgical significance," *Tohoku J. Exp. Med.*, vol. 185, pp. 209–216, Jul. 1998.

[15] L. Kaufman and P. Rousseeuw, *Finding Groups in Data: An Introduction to Cluster Analysis*. New York: Wiley, 1990.

[16] *MATLAB 6.5 Documentation*, The Mathworks, Natick, MA, 2002.

[17] R. L. Ott and M. Longnecker, *An Introduction to Statistical Methods and Data Analysis*. Pacific Grove, CA: Duxbury, 2001.

[18] A. Ridolfi and J. Idier, "Penalized Maximum Likelihood Estimation for Normal Mixture Distributions," Ecole Polytechnique Federale de Lausanne, Lausanne, Switzerland, Tech. Rep. 200 285, 2002.

[19] H. J. Khamis, "The two-stage δ-corrected Kolmogorov–Smirnov test," *J. Appl. Statist.*, vol. 27, pp. 439–450, May 2000.

[20] *The R Environment for Statistical Computing and Graphics: Reference Index*, R Development Core Team, Vienna, Austria, 2003.

[21] F. J. Rohlf and R. R. Sokal, *Statistical Tables*. New York: Freeman, 1995.

[22] *SAS OnlineDoc*, SAS Institute Inc., 1999.

[23] R. N. Rohling and J. M. Hollerbach, "Calibrating the human hand for haptic interfaces," *Presence*, vol. 2, pp. 281–296, 1993.

[24] F. J. Valero-Cuevas, "An integrative approach to the biomechanical function and neuromuscular control of the fingers," *J. Biomech.*, vol. 38, pp. 673–684, Apr. 2005.

[25] J. L. Pearlman, S. S. Roach, and F. J. Valero-Cuevas, "The fundamental thumb-tip force vectors produced by the muscles of the thumb," *J. Orthop. Res.*, vol. 22, pp. 306–312, Mar. 2004.

[26] M. C. Hume, H. Gellman, H. McKellop, and J. R. H. Brumfield, "Functional range of motion of the joints of the hand," *J. Hand Surg. Am.*, vol. 15A, pp. 240–243, Mar. 1990.

[27] G. Ateshian, M. P. Rosenwasser, and V. C. Mow, "Curvature characteristics and congruence of the thumb carpometacarpal joint: Differences between female and male joints," *J. Biomech.*, vol. 25, pp. 591–607, Jun. 1992.

[28] R. Yoshida, H. O. House, R. M. Patterson, M. A. Shah, and S. F. Viegas, "Motion and morphology of the thumb metacarpophalangeal joint," *J. Hand Surg. Am.*, vol. 28A, pp. 753–757, Sep. 2003.

[29] A. Miller, P. Allen, V. J. Santos, and F. J. Valero-Cuevas, "From robotic hands to human hands: A visualization and simulation engine for grasping research," *Ind. Robot.*, vol. 32, pp. 55–63, Jan. 2005.

[30] F. J. Valero-Cuevas and C. F. Small, "Load dependence in carpal kinematics during wrist flexion *in vivo*," *Clin. Biomech.*, vol. 12, pp. 154–159, Apr. 1997.

[31] Y. Bei and B. J. Fregly, "Multibody dynamic simulation of knee contact mechanics," *Med. Eng. Phys.*, vol. 26, pp. 777–789, Nov. 2004.

[32] J. J. Rawlinson, B. D. Furman, S. Li, and D. L. Bartel, "Kinematics, stresses, and damage from a tkr simulator and a finite element model," in *Proc. Orthop. Res. Soc. 47th Ann. Mtg.*, vol. 26, San Francisco, CA, 2001, Paper 0216.

[33] F. J. Valero-Cuevas, N. Smaby, M. Venkadesan, M. Peterson, and T. Wright, "The strength-dexterity test as a measure of dynamic pinch performance," *J. Biomech.*, vol. 36, pp. 265–270, Feb. 2003.

Veronica J. Santos (M'03) received the B.S. degree in mechanical engineering and a music minor from the University of California at Berkeley in 1999, and the M.S. degree in mechanical engineering from Cornell University, Ithaca, NY in 2004. She is currently working towards the Ph.D. degree at the Sibley School of Mechanical and Aerospace Engineering at Cornell University.

From 2000 to 2001, she was a Quality Engineer and Research and Development Engineer at Guidant Corporation in Santa Clara, CA, specializing in life-saving cardiovascular technology. Her research interests include robotics, neural control of movement, and clinical applications of biomechanical modeling, specifically rehabilitation technology and surgical procedures.

Ms. Santos is a member of the IEEE Engineering in Medicine and Biology Society, the American and International Societies of Biomechanics, the American Society of Mechanical Engineers, the Society for the Neural Control of Movement, and the Society of Women Engineers. She has received the Young Investigator Poster Presentation Award from the International Society of Biomechanics (2005), an Exceptional Teaching Assistant Award from the Sibley School of Mechanical and Aerospace Engineering at Cornell University (2005), and a National Science Foundation Graduate Research Fellowship (2001).

Francisco J. Valero-Cuevas (M'02) received the B.S. degree in engineering from Swarthmore College, Swarthmore, PA, in 1988, and the M.S. and Ph.D. degrees in mechanical engineering from Queen's University in Kingston, ON, Canada in 1991 and Stanford University, Stanford, CA, in 1997, respectively.

He is currently Associate Professor at the Sibley School of Mechanical and Aerospace Engineering at Cornell University, Ithaca, NY, and Assistant Scientist at the Musculoskeletal Integrity Program at The Hospital for Special Surgery in New York City. His research interests focus on combining engineering, robotics, mathematics and neuroscience to understand organismal and robotic systems for basic science, engineering and clinical applications.

Prof. Valero-Cuevas is a member of the IEEE Engineering in Medicine and Biology Society, the American and International Societies of Biomechanics, the American Society of Mechanical Engineers, the Society for Neuroscience, and the Society for the Neural Control of Movement. He has received a Research Fellowship from the Alexander von Humboldt Foundation (2005), the Postdoctoral Young Scientist Award from the American Society of Biomechanics (2003), the Faculty Early Career Development Program CAREER Award from the National Science Foundation (2003), the Innovation Prize from the State of Tirol (1999), a Fellowship from the Thomas J. Watson Foundation (1988), and was elected Associate Member of the Scientific Research Society Sigma-Xi (1988). He serves as Associate Editor for the IEEE TRANSACTIONS ON BIOMEDICAL ENGINEERING.